ELSEVIER

Thermochimica Acta 325 (1999) 89–93

thermochimica acta

Mechanism of carbothermal synthesis of aluminium nitride

Pan Wei*, Yang Qing, Cai Juan

Department of Materials Science & Engineering, Tsinghua University, Beijing 100084, People's Republic of China

Received 8 April 1998; received in revised form 9 September 1998; accepted 30 September 1998

Abstract

The reaction between $Al(OH)_3$ and carbon black powders under flowing nitrogen atmosphere was investigated by a dynamic thermogravimetric method. In the temperature range 1300–1700°C, the reaction can be divided into two steps: the first includes the direct reaction between Al_2O_3 and C particles and partial gas–solid reaction at relatively low temperature. The second is the gas–solid reaction between CO–N_2 and Al_2O_3 where the gaseous phase transfers through the cracks in the product layer of AlN to the surface of the un-reacted core of Al_2O_3. The apparent activation energy of the two reactions are 486 and 592 kJ mol^{-1}, respectively. The reaction rates of the two reactions can be expressed as:

$$\frac{d\alpha}{dt} = 8.20 \times 10^{10} \times \exp\left(-\frac{486 \times 10^3}{RT}\right) \times 3 \times (1-\alpha)^{2/3} s^{-1} \text{ (for the first stage)}$$

$$\frac{d\alpha}{dt} = 2.09 \times 10^{13} \times \exp\left(-\frac{592 \times 10^3}{RT}\right) \times (1-\alpha)^{2} s^{-1} \text{ (for the second stage)}$$

Keywords: AlN; Carbothermal nitridation; Dynamic thermogravimetric analysis; Kinetics

1. Introduction

AlN is an attractive material that possesses high intrinsic thermal conductivity (K∼320 W/m K), high electrical resistivity (10^{13}∼10^{16} W m), low dielectric constant and loss, and low thermal expansion coefficient (4.3×10^{-6} to 4.5×10^{-6}/°C) close to that of silicon [1]. The high wear resistance, low density, and high mechanical strength make aluminium nitride a very useful material for both structural and electronic applications [2,3]. Currently, there are various methods for the synthesis of AlN, including direct nitridation of aluminium, carbothermal reduction of Al_2O_3, chemical vapor deposition (CVD), gas-phase synthesis, and preparation from organometallic precursors. Because the carbothermal reduction process can be an economical route for the production of AlN, it has been widely used by many companies such as Tokuyama Soda, Sumitomo Chemical, and Dow Chemical to manufacture AlN powders commercially [4]. While many laboratory investigations have been carried out on this process, only a few attempts have been made to determine the reaction mechanism and the results are inconsistent. For example, Hirai et al. [5] suggested that gas diffusion through the nitride scale is

*Corresponding author. Fax: +86-010-6277-1160;
e-mail: pnaw@mail.tsinghua.edu.cn

0040-6031/99/$ – see front matter
PII: S0040-6031(98)00562-0

the rate-limiting step, whereas Lefort and Billy [6] noted that combustion of carbon controlled the reaction. Hence, it is valuable to clarify the mechanism of the carbothermal reduction process. In this paper, emphasis is focused on the kinetics of the reaction between fine carbon black and $Al(OH)_3$ powders in flowing nitrogen atmosphere. A reaction mechanism based on non-isothermal thermogravimetric analysis is proposed.

2. Experimental

Aluminium trihydroxide ($Al(OH)_3$) (mean particle size: 1.25 μm; purity: 99%) and carbon black (mean particle size: 0.07 μm, purity: 99.9%) powders were mixed in alcohol by ball milling. The molar ratio of $Al(OH)_3$ and carbon was 2/3 according to the stoichiometric equation

$$2Al(OH_3)(s) + 3C(s) + N_2(g) = 2AlN(s) + 3H_2O(g) + 3CO(g) \quad (1)$$

An alumina crucible was used to hold the mixture which was compacted into pellets. The mass change during the reaction was detected by thermogravimetry (TG-DTA92B, Setaram, France). High purity N_2 gas was introduced at a flow rate of 30 ml/min at atmospheric pressure. Simultaneously, gas sampled from the TG furnace during the tests was analysed by a mass analyzer (Finnigan MAT4519). A series of non-isothermal tests were conducted with different heating rates (β=3, 5, 19, 15 K/min) from 1273 to 1973 K. To investigate the effect of temperature on the reaction products, some experiments were carried out in the temperature range 298–1623 and 298–1723 K. Reaction products were analyzed by X-ray diffraction (XRD) and examined by transmission electron microscopy (TEM).

3. Results and discussion

3.1. Results

Fig. 1 shows the typical thermogravimetry (TG) and derivative thermogravimetry (DTG) curves obtained under the heating condition shown. The TG curve contains two stages, with the weight loss

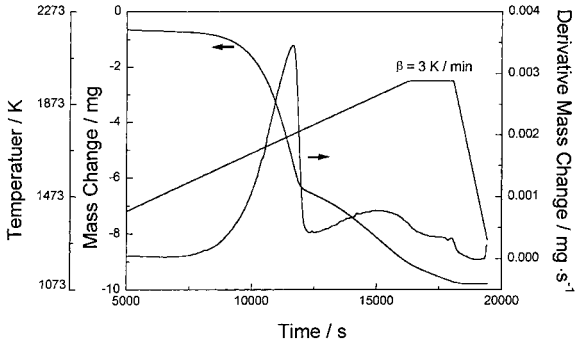

Fig. 1. Typical TG-DTG curves of the Al_2O_3–C mixture in N_2 atmosphere at a heating rate of 3 K min^{-1} in the temperature range of 1273–1973 K, along with the temperature curve in the experiment.

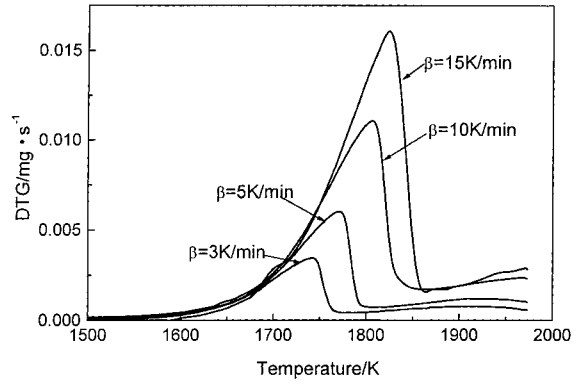

Fig. 2. DTG curves vs. temperature under different heating rates.

rate in the first stage much higher than that in the second. Fig. 2 shows DTG curves at different heating rates. The maximum reaction rate and the peak temperature increase with increasing heating rate. XRD patterns of reaction products are shown in Fig. 3. When samples were held at 1623 K for 2 h, the products included AlN and α, θ-Al_2O_3. When samples were held at 1723 K for 2 h, only AlN and α-Al_2O_3 existed. When the reaction temperature was held at 1973 K for 1 h, only a little α-Al_2O_3 remained in the sample in addition to AlN. XRD patterns of samples under different heating rates showed that firing rate had no effect on the composition of the final products at 1973 K. The gas analysis results show that only N_2 and CO were detectable. The morphology and the electron diffraction pattern of the products from TEM

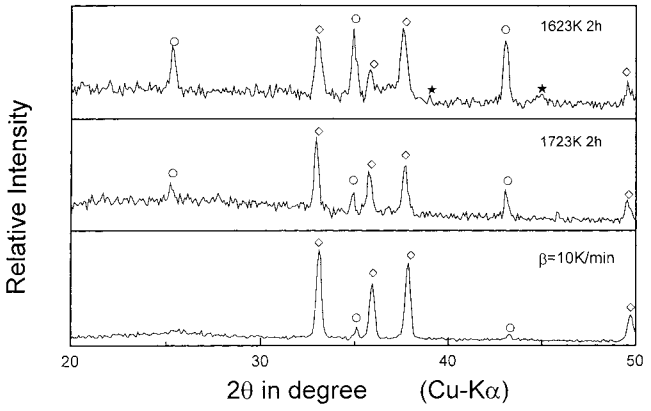

Fig. 3. XRD patterns of the reaction products. (○ α-Al_2O_3, ◇ AlN, * θ-Al_2O_3).

showed that very fine AlN powder (mean size 20 nm) is produced.

3.2. Thermodynamics

Since the aluminium trihydroxide ($Al(OH)_3$) will dehydrate at elevated temperature (below 1000 K) to become the α phase of alumina, reaction (1) can be divided into two separate steps:

$$2Al(OH)_3(s) = Al_2O_3(s) + 3H_2O(g) \quad (2)$$

and

$$Al_2O_3(s)+3C(s)+N_2(g) = 2AlN(s) + 3CO(g) \quad (3)$$

The Gibbs free energy of reaction (3) is [7]

$$\Delta G_3 = 689.9 \times 10^3 - 0.353 \times 10^3 T + RT \ln(p_{CO}^3/p_{N_2})\ \mathrm{J\,mol^{-1}} \quad (4)$$

The starting temperature of the reaction, elevated with increasing heating rate, is in the range 1537–1613 K. Therefore, according to Eq. (4), the equilibrium partial pressure of CO is rather low, ca. 0.02–0.05$\times 10^5$ Pa. At high temperature the reducing ability of CO is enhanced and the following reaction occurs when the alumina particles are not directly in contact with carbon [7]

$$Al_2O_3(s) + 3CO(g) + N_2(g) = 2AlN(g) + 3CO_2(g) \quad (5)$$

$$\Delta G_5 = 190.76 \times 10^3 - 0.1591 \times 10^3 T + RT \ln\left(\frac{p_{CO_2}^3}{p_{CO}^3 p_{N_2}}\right)\ \mathrm{J\,mol^{-1}}$$

$$CO_2(g) + C(s) = 2CO(g) \quad (6)$$

$$\Delta G_6 = 166.38 \times 10^3 - 0.1707 \times 10^3 T + RT \ln\left(\frac{p_{CO}^2}{p_{CO_2}}\right)\ \mathrm{J\,mol^{-1}}$$

Provided that p_{N_2} is much larger than the sum of p_{CO} and p_{CO_2}, the relationships between ΔG, T and the equilibrium pressure of the gas of reaction (5) and (6) are shown in Fig. 4. The zone of $\Delta G<0$ or both reactions is specified in the figure. The area of $\Delta G<0$ is expanded with decreasing equilibrium partial pressure of CO. When $p_{CO_2} \ll p_{CO}$ and $p_{CO} \ll p_{N_2}$, the two reactions can take place at high temperature simultaneously.

3.3. Kinetics

As discussed above, the mechanism of the carbothermal reduction between alumina and carbon black is very complex. At low temperature, the direct contact reaction between the two solids as Eq. (3), may be the dominant reaction. From Fig. 1 during the initial stage of the experiment, the weight change is small and the gas evolution rate was not great. After that, the reaction rate increased rapidly with temperature, so the contact area between the alumina and

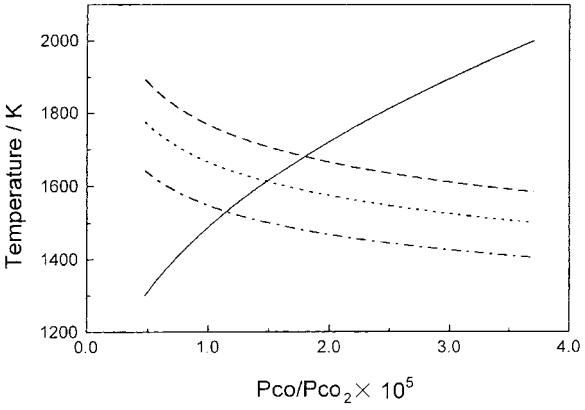

Fig. 4. Relations between ΔG, T and equilibrium partial pressures of gas phases reactants in reactions (5) and (6), assuming $p_{N_2} = 1 \times 10^5$ Pa. ΔG=0 for reaction (5): ———, ΔG=0 for reaction (6): - - - (p_{co}=0.1×10^5 Pa), · · · (p_{co}=0.05×10^5 Pa), -·-·-·- (p_{co}=0.02×10^5 Pa).

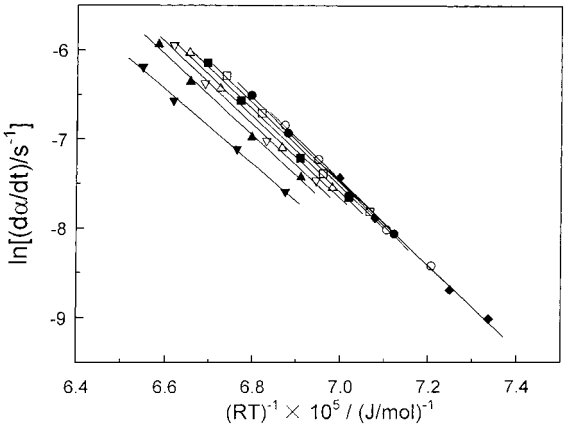

Fig. 5. Plots of ln(dα_1/dt) against (RT)$^{-1}$ for the first stage of the reaction at various values of α_1 from 0.1 to 0.9 in steps of 0.1. (◆ α_1=0.1, ○ α_1=0.2, ● α_1=0.3, □ α_1=0.4, ■ α_1=0.5, △ α_1=0.6, ▽ α_1=0.7, ▲ α_1=0.8, ▼ α_1=0.9.)

carbon black powders would be reduced by the produced gas and the solid–gas reaction expressed by Eqs. (5) and (6) becomes considerable. But the partial pressure of CO_2 was too low to be detected. Fig. 1 also shows that the reaction rate was sharply reduced from the maximum value although the reaction temperature continued to increase. As the reaction proceeded, the AlN product layer formed, surrounding the alumina particle, and acted as a reaction barrier, the reaction determining step changed to diffusion in the AlN layer, and thus the reaction rate decreased sharply. Because the thermal expansion coefficient of alumina (9×10^{-6}/K) is much higher than that of AlN (4.4×10^{-6}/K), as the temperature increased, cracks would be produced in the AlN product layer due to the mismatch in thermal expansion. The reactant gases, CO and N_2, would transfer to the surface of alumina through these cracks, thus the reaction rate of Eq. (5) was increased again at elevated temperature and the second peak of the DTG curve in Fig. 1 appears.

For the kinetic analysis of the TG data, the following formula has been widely applied

$$\frac{\mathrm{d}\alpha}{\mathrm{d}t} = A\exp\left(-\frac{E}{RT}\right)f(\alpha) \tag{7}$$

where α, A, E, R and T stand for the fraction of reaction, frequency factor, apparent activation energy, gas constant and absolute temperature, respectively. To distinguish the fraction of reaction of the first and second stages from that of the whole process, we assumed an α_1 and α_2 calculated by

$$\alpha_\mathrm{i} = \frac{W_\mathrm{oi} - W_\mathrm{fi}}{W_\mathrm{oi}} \tag{8}$$

where W_oi and W_fi are the initial and the end weight of the DTG peaks. Taking the logarithm of Eq. (7) we obtain

$$\ln\left(\frac{\mathrm{d}\alpha}{\mathrm{d}t}\right) = \ln[Af(\alpha)] - \frac{E}{RT} \tag{9}$$

If the form of $f(\alpha)$ does not change with heating rate β, we can use data obtained under various β to calculate the apparent activation energy without knowing the specific form of $f(\alpha)$. The plot of ln(dα/dt) versus (1/T) should yield a straight line from which the E value at a given α can be obtained from the slope. This method was initially proposed by Friedman [8]. The apparent activation energy of both stages was calculated separately. The plots of ln(dα_1/dt) versus $(RT)^{-1}$ at various α_1 are shown in Fig. 5, with the correlation coefficient of the linear regression analysis γ better than −0.9900. An E value of 455±30 kJ/mol was obtained in the range $0.1\leq\alpha_1\leq0.9$. This value is greater than the 384 kJ/mol obtained by Lefort and Billy [6], and less than the 530 kJ/mol by Hirai et al. [5]. Using the same method, we obtained E=624±8 kJ/mol in the range $0.3\leq\alpha_2\leq0.5$ for the second reaction (Fig. 6).

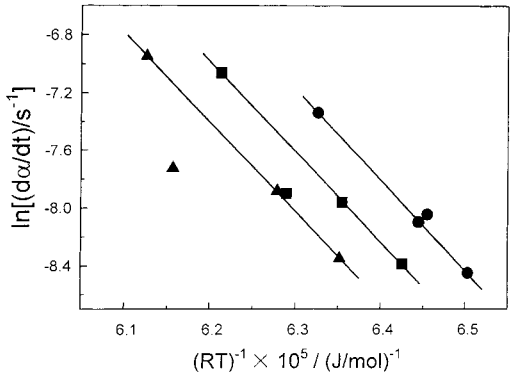

Fig. 6. Plots of $\ln(d\alpha_2/dt)$ against $(RT)^{-1}$ for the second stage of the reaction at various values of α_2 from 0.3 to 0.5 in steps of 0.1 (● α_2=0.3, ■ α_2=0.4, ▲ α_2=0.5).

To determine the kinetic model of the reaction, both differential and integral methods were applied, according to the following equations

$$\ln\left(\frac{d\alpha/dt}{f(\alpha)}\right) = \ln A - \frac{E}{RT} \tag{10}$$

$$\ln(g(\alpha)) = \ln(P(x)) + \ln\left(\frac{AE}{R\beta}\right) \tag{11}$$

where

$$g(\alpha) = \int_0^{\alpha} d\alpha/f(\alpha) \tag{12}$$

$$P(x) = \int_x^{\infty} \frac{e^{-x}}{x^2} dx \text{ and } x = \frac{E}{RT} \tag{13}$$

$$\ln(P(x)) \approx -5.3305 - 1.052x \ (20 < x < 60) \tag{14}$$

and the expressions for $f(\alpha)$ and $g(\alpha)$ depend on the mechanism of the reaction. Many forms of $f(\alpha)$ and $g(\alpha)$ have been developed for reaction mechanisms. Fitting the experimental TG data to these functions, the appropriate kinetic model was selected according to the following criteria: (1) the correlation coefficients γ for both methods are high; (2) the E values are in accord with those obtained by the Friedman method, which is independent of $f(\alpha)$ or $g(\alpha)$. For the first stage, the best fit of $f(\alpha)$ and $g(\alpha)$ are

$$f(\alpha) = 3(1-\alpha)^{2/3} \tag{15}$$

$$g(\alpha) = 1 - (1-\alpha)^{1/3} \tag{16}$$

which are in accord with the phase boundary (spherical symmetry) model and we get E=486 kJ/mol and A=8.02×10^{10}. The overall reaction at the first stage can be expressed as

$$\frac{d\alpha}{dt} = 8.20\times10^{10} \times \exp\left(-\frac{486\times10^3}{RT}\right) \times 3 \times (1-\alpha)^{2/3} s^{-1} \text{ (for the first stage)} \tag{17}$$

As to the second stage, the most appropriate model is

$$\frac{d\alpha}{dt} = 2.09\times10^{13} \times \exp\left(-\frac{592\times10^3}{RT}\right) \times (1-\alpha)^{2/3} s^{-1} \text{ (for the second stage)} \tag{18}$$

which is an empirical function for phase-boundary-controlled reactions [9].

References

[1] I.V. Nicolaescu, G. Tardos, R.E. Riman, J. Am. Ceram. Soc. 77 (1994) 2265.
[2] L.M. Sheppard, Am. Ceram. Soc. Bull. 69 (1990) 1801.
[3] E. Ponthieu, P. Grange, B. Delmon, J. Eur. Ceram. Soc. 8 (1991) 233.
[4] G. Selvaduray, L. Sheet, Mater. Sci. Technol. 9 (1993) 463.
[5] S. Hirai, T. Miwa, T. Iwata, M. Ozawa, H.G. Katayama, J. Japan Inst. Metals 53 (1989) 1035.
[6] P. Lefort, M. Billy, J. Am. Ceram. Soc. 76 (1993) 2295.
[7] E.T. Turkdogan, Physical Chemistry of High Temperature Technology, Academic Press, New York, 1980.
[8] H.L. Friedman, J. Polym. Sci., Part C C6 (1964) 183.
[9] N. Koga, J. Malek, Thermochim. Acta., 282/283 (1996) 69.